

## Cytotoxic effects of a mixed ligand copper(II) chelate complex against a panel of human and murine cancer cells *in vitro*. Theoretical study of the mechanism of biologic action through molecular modelling

G.D. Geromichalos<sup>1</sup>, G.A. Katsoulos<sup>2</sup>, A. Papageorgiou<sup>1</sup>, D.T.P. Trafalis<sup>3</sup>, C.C. Hadjikostas<sup>2</sup>, S.H. Voyatzi<sup>1</sup>, P. Stravoravdi<sup>1</sup>

<sup>1</sup>Symeonidio Research Center, Theagenio Cancer Hospital, Thessaloniki; <sup>2</sup>Department of Chemistry, Aristotle University of Thessaloniki, Thessaloniki; <sup>3</sup>1st Department of Medical Oncology, "Metaxa" Cancer Hospital, Piraeus, Greece

### Summary

**Purpose:** In an effort to discover new compounds with anticancer activity, we have developed a novel copper (II) [Cu(II)] chelate complex with a tridentate ONN-Schiff base ligand and the anion of salicylate and we evaluated the *in vitro* chemosensitivity of various human and murine tumor cell lines by measuring cell growth inhibition. The ultimate goal was to evaluate the existence of a potential antitumor activity of this complex. Beyond the cytotoxic activity assessment of the complex, we aimed at the elucidation of the underlying mechanism of action of this complex and its interactions with biological molecules, carrying out theoretical (quantum-chemical) calculations.

**Materials and methods:** Cells grown in adherence or in suspension in 96-well microplates were exposed to Cu(II) complex for 24, 48 or 72 h. *In vitro* drug cytotoxicity was assessed by SRB and XTT colorimetric assays.

Molecular modelling tools were used applying semiempirical and *ab initio* calculations.

**Results:** A series of experiments was carried out, showing a potent cytotoxic activity against most of the tested cancer cell lines. Quantum-chemical calculations demonstrate that the mechanism of the cellular damage can be explained, at least in part, by the ability of the nucleobases and nucleotides to be subject to nucleophilic attack on copper.

**Conclusion:** Profound growth inhibitory effects were observed for the tested Cu(II) complex. It was also verified the hypothesis that the mechanism of action of this complex involves binding to DNA and RNA. These findings prompt to search for possible interaction of this complex with other cellular elements of fundamental importance for cell proliferation.

**Key words:** cancer, cell lines, copper complexes, Cu(SalNET<sub>2</sub>) salicylate, cytotoxicity, molecular modelling

### Introduction

Since the original discovery of anticancer effects

of platinum compounds, numerous studies have been undertaken to determine what kind of relationships exist between chemical structure and antitumor activity with a view to find out more active drugs. Transition metal complexes with biological activity have gained prominence due to the success of the platinum anticancer drug cisplatin (*cis*-[PtCl<sub>2</sub>(NH<sub>3</sub>)<sub>2</sub>]). To date, several Cu(II) complexes have been tested as potential anticancer agents. Hydrazones of pyridoxal and the structurally related salicylaldehyde are a promising class of compounds, with demonstrated bioactivity. An example is the tridentate ligand salicylaldehyde benzoylhydrazone (H<sub>2</sub>sb), of which Cu(II) complex [Cu(Hsb)Cl]·H<sub>2</sub>O was shown to be a potent inhibitor of DNA synthesis and cell growth and more effective than the

Received 02-09-2004; Accepted 23-09-2004

Author and address for correspondence:

George Geromichalos, PhD  
Theagenio Cancer Hospital  
Symeonidio Research Center  
Laboratory of Cell Culture  
1, Lithoxou street  
551 31 Thessaloniki  
Greece  
Tel: +30 2310898237  
Fax: +30 2310845514  
E-mail: gerom@chem.auth.gr

metal-free chelator [1]. In accordance with this approach, we have directed our efforts towards the biological study of a 4-coordinate Cu(II) chelate complex with a tridentate ONN-Schiff base ligand. We have reported the results concerning the synthesis, structure elucidation, and antineoplastic activity of some novel Cu(II) complexes of the general formula Cu(SalNEt<sub>2</sub>)Y where SalNEt<sub>2</sub> stands for the anion of the N-(2-(diethylamino)ethyl)salicylideneaminato ligand and Y is the anion of a carboxylic or a dicarboxylic acid [2,3]. X-ray structure analysis of Cu(SalNEt<sub>2</sub>)(OCOPh) confirms a slightly distorted square-planar coordination geometry around the copper (paper in preparation).

In our previous studies, chelate complexes of Cu(II) of the general formula Cu(SalNEt<sub>2</sub>)Y, showed exceptional cytotoxic action by inhibiting the proliferation of HeLa-S3 human cervical cancer cells [2]. In another study we have carried out, concerning the examination of the *in vitro* cytotoxicity of the same Cu(II) chelate complexes alone or in combination with various chemotherapeutic drugs in normal and tumor cell lines, it became obvious an important synergistic action in various combinations and in all of the examined cell lines, which action led to increased cytotoxic activity of the examined drugs [3].

In this series of experiments we have focused firstly in the study of the possible anticancer activity of Cu(SalNEt<sub>2</sub>)Salicylate through *in vitro* experiments, and secondly, in the theoretical (quantum-chemical) study of this complex and its adducts with various (deoxy) nucleotides. The ultimate goal was to elucidate the underlying mechanism of action of Cu(II) complex.

Molecular modelling studies are capable to analyze the mechanistic basis for the formation of adducts with DNA and RNA. We tried to correlate the structure of Cu(II) complex and its adducts with biologically active molecules. The theoretical study of the Cu(II) complex and its adducts with various biological molecules was carried out by performing quantum-chemical calculations and aiming at the elucidation of the structure. The purpose was to designate the molecule sites that are subject to nucleophilic or electrophilic attack and finally the correlation of the calculated molecular parameters with the biologic activity of the complex.

## Materials and methods

### Cell lines

The cell lines used were the human cancer cell lines HeLa (cervical) [4], HT29 (colon) [5], OAW-

42 (ovarian) [6], A-549 (lung), MCF-7 and T47D (breast) [7-9], K562 (human myeloid leukaemia) [10], Raji (Burkitt's lymphoma), the murine leukemia L1210 and the normal lung cell line MRC-5. Cells were obtained from the Imperial Cancer Research Found (ICRF), London, and the American Tissue Culture Collection (ATCC).

### Experimental agents

The chemical structure of Cu(SalNEt<sub>2</sub>)Salicylate complex is depicted in Figure 1. Cu-Sal complex was tested in 9 sextuplicate dilutions starting with a peak concentration of 200 μM. Cu-Sal complex was dissolved in DMSO to a concentration of 2 mM. The final concentration of DMSO was less than 0.1%, a concentration that exhibits no effect on cell growth and proliferation, as was experimentally confirmed.

### Cell culture maintenance

Cells were routinely grown as monolayer and suspension cell cultures in T-75 flasks (Costar) in an atmosphere containing 5% CO<sub>2</sub> in air, and 100% relative humidity at 37° C and subcultured twice a week. The culture medium used was either DMEM (for the adherent cells) or RPMI-1640 (for the suspension cells) (Gibco), supplemented with 10% fetal bovine serum (Gibco), 2 mM glutamine (Sigma), 100 μg/ml streptomycin and 100 IU/ml penicillin.

### Drug exposure – XTT and SRB cytotoxicity assays

For the experiments, cells were plated (100 μl per well) in 96-well microplates (Costar-Corning) at

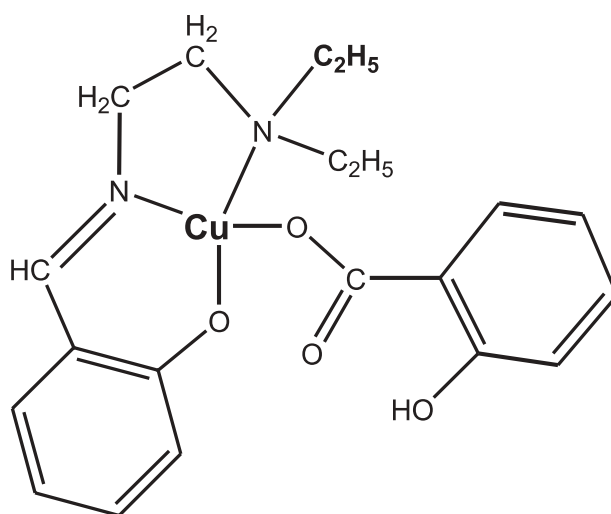


Figure 1. Chemical structure of Cu(SalNEt<sub>2</sub>)Salicylate.

various cell inoculation densities (see legend in Figure 2). Cells were left for 24 h at 37°C to resume exponential growth and afterwards exposed to Cu(II) complex for 24, 48 or 72 h by the addition of an equal volume (100  $\mu$ l) of either complete culture medium (control wells), or twice the final drug concentrations diluted in complete culture medium. Drug cytotoxicity was measured by means of SRB or XTT colorimetric assays estimating the survival fractions (SF) as the percent of control (untreated cells) absorbance. Six replicate wells for each concentration were used for each assay. The colorimetric assays were carried out as previously described [11,12] and modified by our team [13].

### Calculation of results

For each tested compound a dose-effect curve was produced. Sextuplicate determinations gave a coefficient of variation (CV) of much less than 10% (if CV < 10% the results were considered reliable). The data showing inhibition of cellular growth were expressed as the fraction of cells that remained unaffected (fu or SF), which was derived from the following equation:  $fu = OD_x/OD_c$  (where  $OD_x$  and  $OD_c$  represent the test and the control optical density, respectively). Drug potency was expressed in terms of  $IC_{50}$  values (50% inhibitory concentration) calculated from the plotted dose-effect curves (through least-square regression analysis).

### Theoretical calculations

Geometry optimizations were accomplished with semiempirical, *ab initio* (Hartree-Fock), density functional (DFT) and MP2 approaches using different basis sets (STO-3G, 3-21G and 6-31G\*, pBP/DN\*, SVWN/DN\*), as implemented in the MacSpartan Pro suite (MacSPARTAN Pro, 1998, Wavefunction, Inc., Irvine, CA). Using the MacSpartan Pro program package we succeeded in simulating the molecular structures of these compounds and their adducts with various biological molecules.

## Results

Cu-Sal complex has shown a potent cytotoxic activity against a panel of human and murine cancer cell lines. Figures 2 and 3 illustrate the dose-effect plots of various cell lines after 48 or 72 h treatment with Cu-Sal complex. Each point represents the mean of 6 replicate wells. The *in vitro* cytotoxic activity of

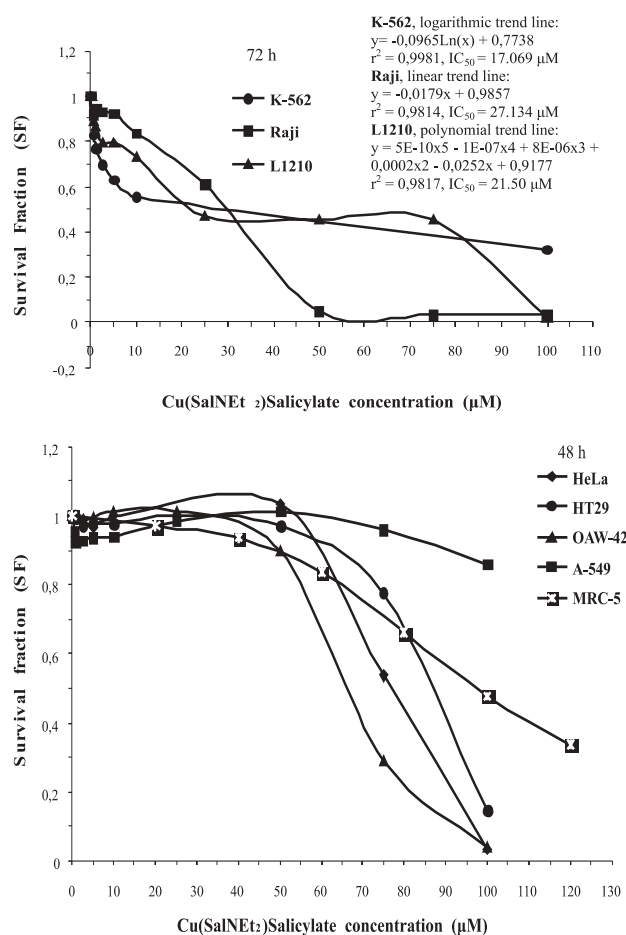


**Figure 2.** Dose-effect curves of Cu-Sal complex against a panel of human and murine cancer cells after 48 & 72 h of treatment. Cytotoxicity was estimated via SRB & XTT assays (cell inoculation densities for adherent cells, HeLa: 5,000 cells/well, HT29, OAW-42, A-549 & MRC-5: 10,000 cells/well with 24 h preincubation period, and for suspension cells, K-562, Raji, L1210: 50,000 cells/well, without preincubation).

this Cu(II) complex seems rather promising. From the derived  $IC_{50}$  values it is concluded that the cytotoxic effect of Cu-Sal on the tested cells was strictly concentration and time-dependent. In Figures 2 and 3 the differences in the chemosensitivity pattern of cells exposed to Cu-Sal complex are demonstrated. Cu-Sal complex was found more active against leukemic and lymphomatic cell lines, exhibiting  $IC_{50}$  values lower than 30  $\mu$ M (17.069  $\mu$ M for K-562 cells, 27.134  $\mu$ M for Raji cells and 21.50  $\mu$ M for L1210 cells) (Figure 2 and Table 1). Table 1 illustrates the  $IC_{50}$  values of the tested agent against the cell lines used. Cu-Sal complex exhibited  $IC_{50}$  values of 4.40, 2.43 and 1.73  $\mu$ g/ml at 24, 48 and 72 h of continuous exposure, respectively, against T47D cells (Figure 3 and Table 1).

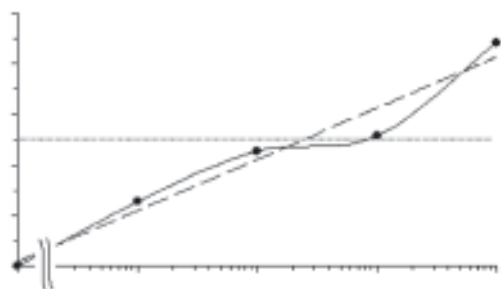


**Figure 3.** Chemosensitivity of T47D human breast cancer cells (24 h preincubation of cells without drug at a cell inoculation density of 10,000 cells/well) against Cu-Sal complex after 48 h of continuous exposure (XTT assay).

T47D cells were the most sensitive over the action of Cu-Sal complex with an  $IC_{50}$  value of 10.489, 5.793  $\mu\text{M}$  and 4.052 at 24, 48 and 72 h, respectively, of continuous exposure. At the same time Cu-Sal complex exhibited a decreased cytotoxicity on all other cells with  $IC_{50}$  values shown on Table 1, indicating a 13-fold decrease in sensitivity (for HeLa), 15-fold (for HT29), 11.4-fold (for OAW-42), 16.9-fold (for MRC-5) and >17-fold (for A-549) 48 h after administration of the agent, 4.6-fold (for MCF-7) 24 h after drug administration and 4.2-fold (for K-562), 6.7-fold (for Raji) and 5.3-fold (for L1210) 72 h after drug administration. It is apparent that Cu-Sal complex had a minor effect on A-549 ( $IC_{50} > 100 \mu\text{M}$ ).

Furthermore, among leukemia and lymphoid cell lines, K-562 cell line was the most sensitive to Cu-Sal

**Table 1.** Chemosensitivity of various cell lines to Cu-Sal complex expressed in  $IC_{50}$  values, after 24, 48 or 72 h of continuous exposure (SRB and XTT assay)

Cell line	$IC_{50}$ ( $\mu\text{M}$ ) 24h	$IC_{50}$ ( $\mu\text{M}$ )	
		48h	72h
T47D	10.489 <sup>†</sup>	5.793 <sup>†</sup>	4.052 <sup>†</sup>
MCF-7	27.20 <sup>†</sup>	ND	18.80 <sup>†</sup>
HeLa	ND	76.50 <sup>‡</sup>	ND
HT29	ND	87.00 <sup>‡</sup>	ND
OAW-42	ND	66.20 <sup>‡</sup>	ND
A-549	ND	> 100.00 <sup>‡</sup>	ND
MRC-5	ND	98.00 <sup>‡</sup>	ND
K-562	ND	ND	17.07 <sup>†</sup>
Raji	ND	ND	27.13 <sup>†</sup>
L1210	ND	ND	21.50 <sup>†</sup>

<sup>†</sup>XTT assay, <sup>‡</sup>SRB assay, ND: not done

complex, 72 h after drug treatment, with  $IC_{50}$  value of 17.07  $\mu\text{M}$ , compared to corresponding  $IC_{50}$ 's of 27.13  $\mu\text{M}$  and 21.50  $\mu\text{M}$  for Raji and L1210 cells, respectively (Table 1). As depicted in Figures 2 and 3 or Table 1, the order of cell sensitivity was as follows: T47D > K-562 > MCF-7 > L1210 > Raji > OAW-42 > HeLa > HT29 > MRC-5 > A-549. To test whether the effect of Cu(II) complex could be attributed to the salicylate ligand or not, we tested the effect of the ligand alone against T47D cell line. The ligand exhibited only a negligible inhibition of cellular proliferation (data not shown).

The molecular structure and several parameters related to chemical reactivity and biological behavior and activity of the Cu-Sal complex adducts with 3'-dNMP (monodentate interaction) and 5'-GMP and 5'-CMP (bidentate attack with the formation of a closed macrochelate ring) were investigated. The smaller the energy of the Highest Occupied Molecular Orbital (HOMO) of the nucleotide, the bigger the energy difference from the Lowest Unoccupied Molecular Orbital (LUMO) of the Cu(II) complex ( $\Delta E_{\text{LUMO-HOMO}}$ ), and consequently the interaction between the frontier orbitals (this means more difficult nucleophilic attack of the nucleotide on Cu(II) complex) will be more difficult. From Table 2 the following order of energy decrease between DNA and RNA nucleotides is derived: 5'-CMP > 5'-dGMP > 5'-dAMP > 5'-AMP > 5'-GMP > 5'-dCMP > 5'-TMP > 5'-UMP, for 5'-NMP and 3'-dGMP > 3'-GMP > 3'-dAMP > 3'-AMP > 3'-TMP > 3'-dCMP > 3'-UMP > 3'-CMP for 3'-NMP. The comparison of the RNA nucleotides' (both 3'- and 5'-NMP) HOMO energy resulted in the following order: **3'-GMP** > 5'-CMP > 5'-AMP > 3'-AMP > 5'-GMP > 3'-UMP  $\approx$  5'-UMP > 3'-CMP, while the order for DNA nucleotides' HOMO energy was: **3'-dGMP** > 5'-dGMP > 5'-dAMP > 3'-dAMP > 5'-dCMP > 3'-TMP > 5'-TMP > 3'-dCMP.

Among the RNA nucleotides, 3'-GMP (guanylic acid) will most probably interact with Cu(II) complex since it presents the highest HOMO energy (smaller energy gap), followed by 5'-CMP (5'-cytidilic acid), whilst 3'-CMP (uridylic acid) seems to be less active in attacking Cu(II) complex (lowest HOMO energy) (Table 2). Likewise, among the DNA nucleotides, 3'-dGMP (3'-deoxyguanylic acid) proved to be the most efficient in approaching the electrophilic center of the Cu(II) complex (highest HOMO energy), followed by 5'-dGMP (Table 2). (For the 3'-dCMP – 3'-deoxycytidyl-ic acid, it will be more difficult to approach the electrophilic center of Cu(II) complex since it presents the lowest HOMO energy).

Conclusively, the most drastic in nucleophilic attacks over the Cu atom were the monophosphate

**Table 2.** HOMO energies of 5'- and 3'- nucleotides/deoxynucleotides and energy gap from the LUMO energy of Cu-Sal complex (calculations based on PM3 method)

5'-NMP & 5'-dNMP	$E_{HOMO}$ (eV)	$\Delta E_{LUMO^*-HOMO^{**}}$ (eV)		$E_{HOMO}$ (eV)	$\Delta E_{LUMO^*-HOMO^{**}}$ (eV)
		*LUMO of Cu(SalNEt <sub>2</sub> )Salicylate **HOMO of 5'-NMP or 5'-dNMP	of 3'-NMP & 3'-dNMP		
5'-GMP	-9.063	8.201	3'-GMP	-8.764	7.901
5'-AMP	-9.012	8.150	3'-AMP	-9.037	8.175
5'-CMP	-8.806	7.944	3'-CMP	-9.716	8.854
5'-UMP	-9.619	8.757	3'-UMP	-9.612	8.750
5'-dGMP	-8.947	8.085	3'-dGMP	-8.671	7.809
5'-dAMP	-8.966	8.104	3'-dAMP	-9.024	8.162
5'-dCMP	-9.136	8.273	3'-dCMP	-9.525	8.663
5'-TMP	-9.311	8.445	3'-TMP	-9.191	8.329

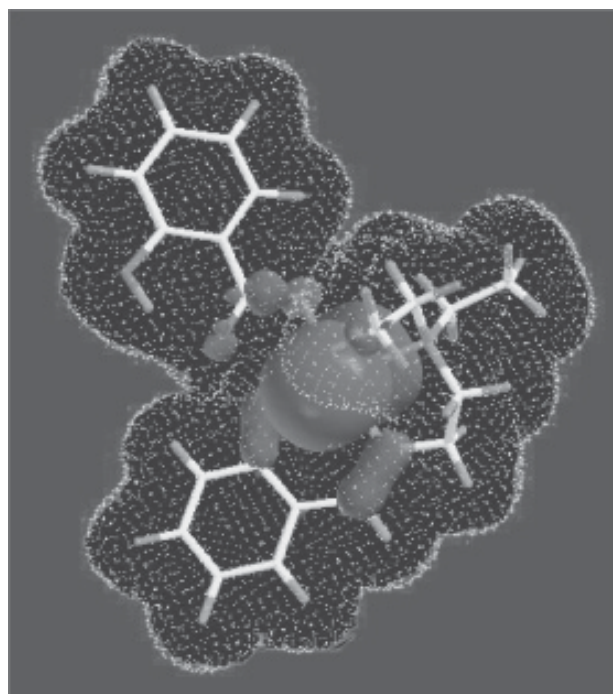
nucleotides of guanosine, followed by the corresponding nucleotides of adenosine.

Figure 4 illustrates the isodensity surface and the LUMO orbital of the Cu-Sal complex optimized structure on which *ab initio* calculations have been performed. The LUMO orbital, which delineates the areas most electron-deficient in a molecule, (hence subject to nucleophilic attack), is localized on Cu atom and indicates where the next pair of electrons from the HOMO orbital of the nucleotide will go, coordinating with Cu the way through the newborn bond (the atom where the LUMO is more heavily localized, is more reactive toward attack by a nucleophile).

From Figures 5 and 6 it is obvious that the HOMO orbital is localized more or less on atoms N<sub>7</sub>, N<sub>1</sub>, N<sub>3</sub>, C<sub>4</sub>, C<sub>5</sub> and C<sub>8</sub>, the sp<sup>3</sup>N of -NH<sub>2</sub> group and on atoms O<sub>6</sub> and N<sub>9</sub>. In 5'- and 3'-(d)GMP, the localization is shown mainly on atoms N<sub>7</sub>, N<sub>3</sub> and C<sub>4</sub>, C<sub>5</sub> and C<sub>8</sub> and to a lesser degree on N<sub>1</sub>, N<sub>9</sub>, the N of -NH<sub>2</sub> group, and the O<sub>6</sub>. In 5'- and 3'-(d)UMP, the HOMO orbital is located mainly on atoms N<sub>1</sub> and N<sub>3</sub> and to a lesser degree on the N of -NH<sub>2</sub> group. Specifically, in the 5'-dCMP the localization is apparent mainly on atoms C<sub>5</sub>, C<sub>6</sub> and in O<sub>2</sub> (not all data are shown).

In Figure 5 the localization of the electrostatic potential, mainly over the atoms O of phosphate groups and N7 of 5'-GMP, is shown. This indicates that these atoms are subject to electrophilic attack.

Likewise, the localization of electrostatic potential, mainly over the atoms O of phosphate groups and N3 of 5'-CMP, is obvious (Figure 6).



**Figure 4.** Isodensity surface (dots) and Lowest Unoccupied Molecular Orbital (LUMO) (solid) of Cu(SalNEt<sub>2</sub>)Salicylate complex (based on *ab initio* UHF/STO-3G quantum-chemical calculations).

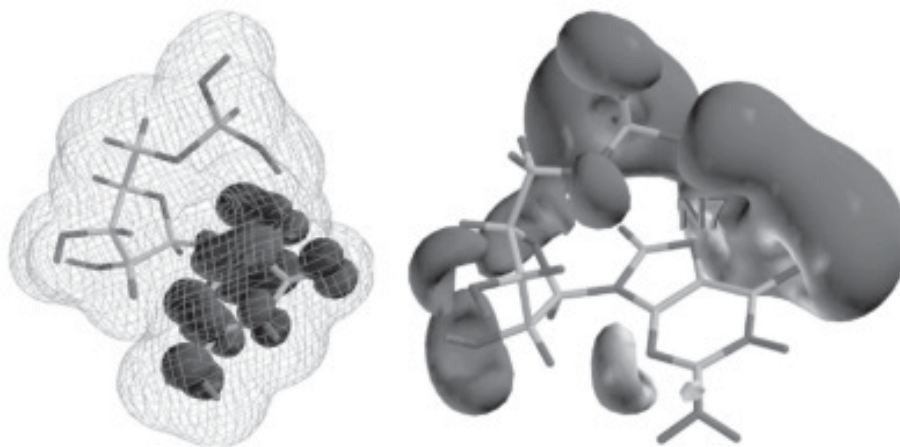


**Figure 5.** Illustration of HOMO frontier molecular orbital of 5'-GMP (solid) at the same time with isodensity surface (mesh) (left) and the electrostatic potential map (electrostatic potential surface on top of which have been color-mapped the values of the HOMO orbital) of the nucleotide (solid), based on PM3 calculations.

The molecular and electronic structure of the adducts of the Cu-Sal complex with various 3'-deoxynucleotides through a monodentate interaction [3'-dGMP (deoxyguanylic acid), 3'-dAMP (deoxyadenylic acid), 3'-TMP (thymidylic acid), 3'-dCMP] and also through a bidentate attack with various 5'-nucleotides like 5'-GMP (guanylic acid) and 5'-CMP (cytidylic acid) were also investigated and are illustrated in Figures 7 and 8. The adduct formation is produced through the creation of a closed macrochelate ring. The geometry around Cu(II) is a distorted octahedral. Figure 7 presents the optimized molecular structure of Cu-Sal complex adduct with 5'-GMP (guanyl-

ic acid) in which the close of the macrochelate ring is achieved through the attack to Cu from N7 and the O of guanine. On the right are shown the surfaces of HOMO and LUMO orbital in the same time with the spin chart. In Figure 8 the same structures and surfaces for the adduct of Cu-Sal complex with 5'-CMP (cytidylic acid) are illustrated.

## Discussion

The purpose of these experiments was to study the chemosensitivity pattern of human and murine

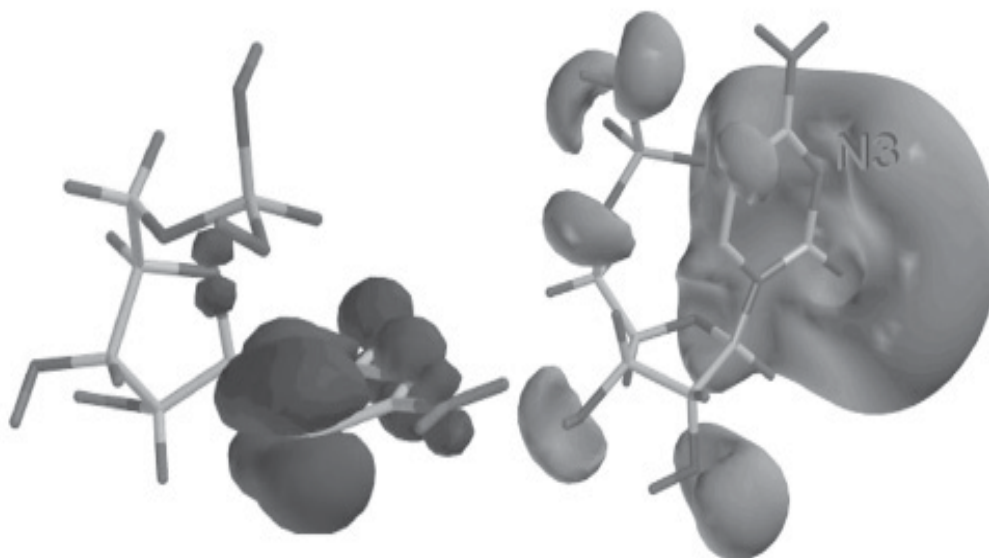


**Figure 6.** Illustration of HOMO frontier molecular orbital of 5'-CMP (solid) at the same time with isodensity surface (mesh) (left) and the electrostatic potential surface of the nucleotide (solid), based on PM3 calculations.



**Figure 7.** Molecular structure of the adduct  $\text{Cu}(\text{SalNet}_2)\text{Salicylate}(5' \text{-GMP})\text{N7},\text{O}_{\text{pi}}\text{-cl}$  (left) and illustration of the frontier molecular orbitals HOMO (solid) and LUMO (transparent) in the same time with spin chart (mesh) (right), based on PM3 calculations (formation of a closed (cl) macrochelate ring through nucleophilic attack on Cu from N7 and the O of the phosphate group,  $\text{O}_{\text{pi}}$ ).

cancer cells. We conclude that the Cu-Sal complex proved active against almost all tested cell lines. From cancer cell lines, both human breast (T47D and MCF-7) and erythroleukemia (K-562) cells appeared to be

the most susceptible at 72 h of continuous exposure to Cu-Sal, while human lung tumor cells were the more resistant. An intermediate chemosensitivity was defined for the rest of the solid human tumor cells after

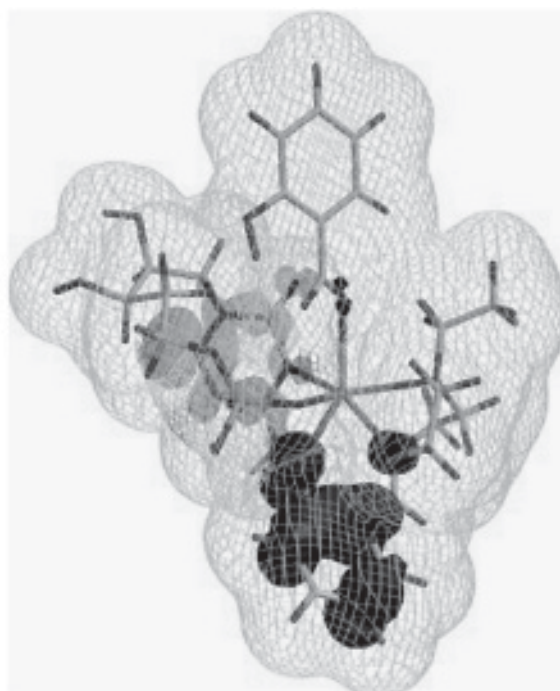


**Figure 8.** Molecular structure of the adduct  $\text{Cu}(\text{SalNet}_2)\text{Salicylate}(5' \text{-CMP})\text{N3},\text{O}_{\text{pi}}\text{-cl}$  (left) and illustration of the frontier molecular orbitals HOMO (solid) and LUMO (transparent) in the same time with spin chart (mesh) (right), based on PM3 calculations (formation of a closed (cl) macrochelate ring through nucleophilic attack on Cu from N3 and the O of the phosphate group,  $\text{O}_{\text{pi}}$ ).

the administration of Cu-Sal, exhibiting  $IC_{50}$  values at least 4-fold higher compared to more sensitive cells.

Experimental results indicate that normal and tumor cells respond differently to changes of environmental conditions, which are suboptimal for growth. It should be kept in mind that since tumor cells revealed to be more sensitive than normal cells (MRC-5), taking also into account the heterogeneity of response between different tumor cell populations, the growth inhibitory effects could be attributed to cytostatic activity of the compound than to non-specific cytotoxicity, although exceptions might exist. A more reliable tool for distinguishing between these actions is measuring the DNA synthesis [14].

Quantum-chemical methods of computational chemistry have allowed us to simulate the molecular structures of Cu-Sal complex and its adducts with biological molecules. The mechanism of the cellular damage can be explained, at least in part, by the ability of the nucleobases and nucleotides to be subject to nucleophilic attack on Cu-Sal complex. The results supported our hypothesis that the mechanism of action of this complex involves binding to DNA and RNA. These findings prompt to search systematically for the possible interaction of the complex with other cellular elements, which are of fundamental importance in cell proliferation.

There is considerable interest in the DNA binding of metal complexes because of their potential applications as DNA probes and as possible antitumor agents [15,16]. A large number of antitumor drugs interact with DNA and cause scission on the DNA [17,18]. Many of the antitumor drugs are inhibitors of nucleic acid synthesis and interact with DNA by an intercalative or a non-intercalative way. Coordination of Cu-Sal to major or minor DNA grooves can be achieved through interstrand and intrastrand linkage. The negatively charged ribose-phosphate backbone of the major and minor grooves of double-stranded DNA and RNA plays host to a variety of positively charged species (as metals, ligands and protein side chains). This type of coordination causes a competitive inhibition of the formation of the typical Watson-Crick hydrogen bonds in the double-stranded DNA. This type of coordination may interrupt the hydrogen bonds between the base pairs leading to an alteration of the regular helical configuration of the two sugar-phosphate backbones. It has been suggested that the unique properties of interstrand cross-links of bifunctional transition metal complexes and the resulting conformational alterations in DNA, have critical consequences for their antitumor effects.

## Conclusion

We conclude that cells appeared to be sensitive to Cu-Sal complex treatment. It was also verified, through theoretical calculations, the hypothesis that the mechanism of action of this complex involves binding to DNA and RNA. These findings prompt to search more systematically for the possible interaction of the complex with other cellular elements, which are of fundamental importance for cell proliferation. A quantitative structure activity relationship (QSAR) study of the compounds should be considered for the understanding and determination of the factors which are responsible for producing the observed cytotoxicity of Cu-Sal complex (bioactivity), for the evaluation of the importance of the copper ion for activity, and for the optimization of the desired biological properties.

Additional work to examine the interaction pattern of the type  $Cu(SalNEt_2)_2Y$  Cu(II) complexes with other biological molecules may be informative. This line of investigation may provide hints about the underlying mechanism of action.

## References

1. Pickart L, Goodwin WH, Burgua W, Murphy TB, Johnson DK. Inhibition of the growth of cultured cells and an implanted fibrosarcoma by aroylhydrazone analogs of the Gly-His-Lys-Cu(II) complex. *Biochem Pharmacol* 1983; 32: 3868-3871.
2. Geromichalos GD, Katsoulos GA, Hadjikostas CC, Kortaris AH, Kyriakidis DA. In vitro synergistic effect of some novel Cu(II) complexes in combination with epirubicin and mitomycin C against HeLa-S3 cervical cancer cell line. *Anticancer Drugs* 1996; 7: 469-475.
3. Geromichalos GD, Katsoulos GA, Hadjikostas CC, Kortaris AH, Kyriakidis DA. In vitro combination effect of a new series of copper(II) complexes with cisplatin or epirubicin on human breast and cervical cancer cell lines. *Drugs Experim Clin Re-s* 1998; 24: 93-104.
4. Gey GO, Coffman WD, Kubicek MT. Tissue culture studies of the proliferative capacity of cervical carcinoma and normal epithelium. *Cancer Res* 1952; 12:264-268.
5. Fogh J, Trempe G. New human tumor cell lines. In: Fogh J (ed): *Human tumor cell lines in vitro*. New York: Plenum Press, 1975, pp 115-159.
6. Wilson AP. Characterization of a cell line derived from the ascites of a patient with papillary serous cystadenocarcinoma of the ovary. *J Natl Cancer Inst* 1984; 72:513-521.
7. Soule HD, Vazquez J, Long A. A human cell line from a pleural effusion derived from a breast carcinoma. *J. Natl Cancer Inst* 1973; 51:1409-1416.
8. Engel LW, Young NA, Tralka TS. Establishment and characterization of three new continuous cell lines derived from human breast carcinoma. *Cancer Res* 1978; 38:3352-3364.
9. Keydar I, Chen L, Karby S et al. Establishment and charac-



- terization of a cell line of a human breast carcinoma origin. *Eur J Cancer* 1979; 15:659-663.
10. Klein E, Ben-Bassat H, Neumann H et al. Properties of the K562 cell line derived from a patient with chronic myeloid leukemia. *Int J Cancer* 1976; 18:421-431.
  11. Scudiero DA, Shoemaker RH, Paull KD. Evaluation of a soluble tetrazolium/formazan assay for cell growth and drug sensitivity in culture using human and other tumor cell lines. *Cancer Res* 1988; 48:4827-4833.
  12. Skehan P, Storeng R, Scudiero D et al. New colorimetric cytotoxicity assay for anticancer screening. *J Natl Cancer Inst* 1990; 82:1107-1112.
  13. Papazisis KT, Geromichalos GD, Dimitriadis KA, Kortsaris AH. Optimization of the sulforhodamine B colorimetric assay. *J Immunol Methods* 1997; 208:151-158.
  14. Wilson AP. Cytotoxicity and viability assays. In: Rickwood D, Hames BD, Freshney RI (eds): *Animal cell culture; a practical approach*. Washington DC, Oxford, IRL Press, 1986, pp 191-204.
  15. Sigel A, Sigel H. Photolytic covalent binding of metal complexes to DNA. In: Billadeau MA, Morrison H (eds): *Metal Ions in Biological Systems*. New York: Dekker, 1996, vol 33, pp 269-282.
  16. Carter DC, He XM. Structure of human serum albumin. *Science* 1990; 249: 302-303.
  17. Ross WE, Glaubiger DL, Kohn KW. Protein associated DNA breaks in cells treated with adriamycin or ellipticine. *Biochim Biophys Acta* 1978; 519: 23-30.
  18. Waring MJ. DNA modification and cancer. *Ann Rev Biochem* 1981; 50: 159-192.